United States
Environmental Protection
Agency

Healt Effects Research
Laboratory
Research Triangle Park NC 27711

Research and Development

EPA/600/S1-87/003 Aug. 1987

EPA

Project Summary

Specific Absorption Rate Distributions in a Heterogeneous Model of the Human Body at Radio Frequencies

Stanislaw S. Stuchly

The electric field distribution or the rate of energy absorption referred to as the specific absorption rate (SAR) in a biological body is a complex function of several exposure parameters such as frequency, intensity of the incident field, polarization, source to object configuration (near-field vs far-field) and the body characteristics such as size, shape and dielectric properties. An experimental approach was employed to determine SAR patterns in a full-scale heterogeneous model of man exposed to radio-frequency fields at 160, 350 and 915 MHz in the far and near fields for two polarizations. The model had an anatomically correct shape and contained a skull, spinal cord, rib cage and all major bones (except those in the feet and hands), brains, lungs and muscle tissue. The square of the electric field inside the model was measured by a small diameter electric field probe. Data acquisition, exposure conditions and data processing were under computer control. Special circuitry including an optical link was used to interface the electric field probe with the computer. Extensive data were obtained, analyzed and compared with the data for a homogeneous model.

This Project Summary was developed by EPA's Health Effects Research Laboratory, Research Triangle Park, NC, to announce key findings of the research project that is fully documented in a separate report of the same title (see Project Report ordering information at back).

Introduction

The electric field distribution or the specific absorption rate (SAR) distribution in a biological body is a complex function of several exposure parameters such as frequency, intensity of the incident field, polarization, source to object configuration, presence of other objects nearby (ground plane, reflectors), and the body parameters such as size, shape and the dielectric properties. To quantify the interactions between RF fields and biological systems both theoretical and experimental dosimetry methods have been developed. A few numerical techniques have been used such as the method of moments, finite-difference method, fast-Fourier transform method and time-domain finite difference method to determine SAR distributions in simplified models of the human body. The main limitation of all the methods is the computer memory and time required, if a reasonable spatial resolution and accuracy are to be achieved.

Experimental dosimetry has been developing in parallel and frequently in conjunction with theoretical dosimetry for the following specific applications: verification of theoretical predictions, determination of the total dose rate (total SAR) in experimental animals, determination of the average SAR and its distribution in models more closely resembling real biological bodies than those treatable theoretically, determination of the SAR in models and animals exposed in the near field under the conditions for which a theoretical analysis is prohibitively dif-

ficult. Experimental dosimetry has been performed on full size models and animals, and on scaled down models (frequency and dielectric properties).

A computer-controlled system recently developed at the University of Ottawa facilitates the effective use of implantable electric field probes to obtain spatial distribution of the electric field and the SAR in full-scale models of humans.

The overall performance of the system was evaluated by measuring the SAR distributions in homogeneous lossy spheres and cylinders at various frequencies of interest using three types of the electric field probes and by comparing the results with the theoretical values.

The system was used to determine spatial distributions of the SAR in a full-scale homogeneous model of man exposed in the far-field at 160 MHz, 350 MHz and 915 MHz and in the near-field of a resonant dipole, a resonant dipole with reflector and a resonant slot.

The objective of the project was to extend the previously developed experimental dosimetry method to a more realistic, heterogeneous model of man, and to determine the spatial distribution of the electric field and the SAR in such a model at selected frequencies.

The objective of the project was met through the following developments:

- development of tissue-equivalent materials to simulate electrical properties of bones, lungs, and brain,
- development and manufacture of a heterogeneous model of man,
- development of a method of probing the electric field in the heterogeneous model (mechanical and electromagnetic aspects),
- evaluation of electric field probe responses in materials having inhomogeneous dielectric properties (the permittivity of bone is an order of magnitude different from that of muscle), in particular close to the boundary between air and high water content tissues,
- acquisition and analysis of the distributions of the SAR at selected frequencies.

Procedure

The experimental system developed in our laboratory consists of a scanning system with an electric field probe, a radiating antenna and a model of a human body in which electric fields strengths are measured. This part of the system is placed in an anechoic chamber to avoid reflections of the radiated RF energy.

The mechanical structure used for supporting the positioning of the electric field probe consists of three custom-made independent guiding slides forming an XYZ-coordinate system. All slides use a lead-screw arrangement.

The probe can be placed at any location within a regular solid of 1.9 x 0.5 x 0.45 m. The dimension of the rectangular volume can be altered by repositioning limit switches at the end of each slide.

The system can operate in a manual or a computer-supervised mode. In the manual mode the probe motion is controlled by switches on a portable, hand-operated unit in order to select probe coordinates that are stored in a file in the minicomputer memory, thus producing a map of measurement points.

In the computer-supervised mode the probe automatically scans through all points of the previously selected map, and the corresponding values of the electric field strength for each position are recorded. After completing the data acquisition phase, the computer can display the results in graphical form on a CRT screen or they can be printed in tabular form on a line printer.

The software used in the data collection and analysis consists of three programs developed for this application and a software package purchased for display of contour and mesh views of the data. The first program called MAP is used in conjunction with the hand-held control unit driving the scanning system to generate a map of coordinates. The second program called SCAN uses this map to automatically take electric field measurements at all of the stored locations. For each location the electric field strength is measured five times and averaged. The same program also controls a digital attenuator that is used to adjust the power to the antenna, in order to keep the signal from the amplifier in a linear range. Each x,y,z location and the associated electric field strength are stored in a disk file. The third program called CHART allows one to display or plot a graph of, for instance, the electric field strength vs. distance (x,y,z). Software developed by Data Plotting Services called DPICT* provides the capability of displaying the electric field strength or SAR, in the form of a contour diagram of equipotential lines or as a 3-dimensional representation.

The electronic circuitry which interfaces the probe output to the computer consists of three FET input amplifiers, a summing junction, an active filter, RMS to DC converter, a voltage to frequency converter, a line driver, a LED and an optical-fiber link to the computer. The optical fiber link brings the signal from the amplifier out of the anechoic chamber to a circuit containing a fiber optic receiver and a frequency to voltage converter. This voltage, which represents the electric field, is then sent to the PDP 11/34 where an A/D converter inputs the signal to the computer.

The overall system capabilities can be summarized as follows:

(1) the SAR measurements repeatability is better than ± 0.5 dB (~10%) (tested on 15 runs under various exposure conditions), and

(2) the SAR measurement uncertainty is ± 1 dB; the main factor is the uncertainty in the probe calibration.

The model of the human body was exposed to RF radiation, from resonant dipole or resonant dipole antennas with reflectors, incident from the front for the far- and the near-field exposures.

For exposures in the far-field, the human model was placed at a distance sufficiently large to ensure the far-field conditions. A complete map of the power density at the plane of the model of man was obtained for a given placement of the source without the model in place. The correction for the nonplanar wave front (amplitude only) was incorporated into the computer program that normalized the measured SAR values to 1 mW/cm^2 of the incident power uniform at the plane of the model of man.

A nonperturbing, implantable electric field probe consisting of a very short dipole and a miniature Schottky-barrier diode connected by high-resistance leads with the external circuitry was designed, constructed and evaluated. The dipoles and the high-resistance leads were deposited on a dielectric substrate. Three dipoles were arranged in a triangular configuration to provide an isotropic directional response. The external diameter of the probe was 1 cm. The output from the Schottky-barrier diode was connected to the electronic circuitry by high-resistance leads with a resistivity of 2 MΩ/m, and a length of 0.3 m.

The probe was calibrated at three frequencies (160, 350 and 915 MHz). The sensitivity of the probes in tissue material was determined by measuring the output voltages of the electric field probe placed at various locations in a sphere made of styrofoam and filled with a dielectric medium having the same

* Mention of trademarks or commercial products does not constitute endorsement or recommendation for use.

dielectric properties as tissue. The output signal was compared (using the least-square fit method) with theoretical values of the electric field in the same locations. The sphere was irradiated by a plane wave of a known power density.

One of the major research objectives was to produce a realistic model of a man which replicated the major anatomical components of the human body. The components chosen were muscle, brain, lung and bone since they have dissimilar dielectric properties. Muscle simulating material was used to model all of the other organs of the body since their properties are similar to muscle (± 10%). The shape of the body was formed by a thin shell into which the components were placed.

The shell was formed by wrapping an Alderson Nuclear Medicine model of the human body in a water-activated casting tape from 3M company. This model was anatomically correct and of the dimensions of a male 1.62 m tall. After setting, the cast was removed from the Alderson Phantom and coated with fiberglass resin. This produced a hard, watertight shell in the shape of a man. The cavity for the lungs was formed in the same way using a plastic model of the lungs. The bones were cast from a material simulating the properties of live human bone using molds from the bones of a skeleton. The interior of the skull was used to form the brain cavity. The lungs were filled with lung-equivalent material, skull with brain-equivalent material and the remaining part of the shell with muscle-equivalent materials.

The components of the muscle material were water, hydroxyethylcellulose (HEC), a compound to increase the viscosity, sodium chloride (NaCl), to increase the conductivity, sucrose to decrease the dielectric constant and a bactericide to prevent breakdown of the polymer by bacterial agents.

The properties of brain tissue were similar to those of skeletal muscle and the same components, in different proportions.

The basis of the lung simulation was the same as the skeletal muscle but with an addition of hollow silica microspheres.

The bone simulating material was made from Devcon Two Ton epoxy to which had been added a highly conductive potassium chloride (KCl) solution. The concentration of the salt solution (electrolyte) was adjusted to vary the conductivity. The electrolyte was incorporated into the epoxy, thus forming ionic conductance carriers in the bone equivalent material.

The dielectric properties of the tissue simulating materials were measured using an open-ended coaxial-line sensor and a computer-controlled automatic network analyzer. The uncertainty of the measurements was determined to be less than 3 percent for the dielectric constant and 2 percent for the conductivity for the muscle, brain and lung materials, and less than 5 and 10 percent for the dielectric constant and conductivity, respectively, for bone simulating material.

The exterior body dimensions and the dimensions and placement of the interior structures were determined by the use of two techniques: laser and CT scans.

An experimental system developed by Hymarc Engineering (Ottawa, Ontario, Canada) in conjunction with the National Research Council of Canada was used to acquire the exterior coordinates of the model. The system accomplishes this task by scanning the model surface with a laster light. This data in the form of x, y, z coordinates was recorded on a floppy disk and then transferred to a VAX 750 computer system to produce a 3-D view of the exterior of the model.

A CT-scanner was used to take scans at 1 cm intervals of the head, neck and upper body and at 10 cm intervals of the legs. The X-ray films were transferred to paper by making contact prints. These pictures defined the location and dimensions of the interior structure of the model.

Results and Discussion

Far-Field Exposure

Thirty-eight locations within one half of the model were selected as measurement sites.

In the far-field and for the E-polarization, high local SARs are produced in the neck at all three frequencies measured (160, 350, 195 MHz). The highest SAR value is at 160 MHz, and a substantially lower SAR value is measured at 915 MHz. The SAR patterns observed in the mid-plane of the model were found to be similar for all frequencies. Much lower SARs were produced at the lowest two test frequencies, namely 160 and 350 MHz for the H-polarization of the incident wave. This is not surprising in view of the lower total whole body SAR deposited for the H-polarization as compared with the E-polarization. At 915 MHz, for the H-polarization only, somewhat lower SARs in the neck were produced as compared with the E-polarization. This again could be explained by comparable whole-body SARs at this frequency.

The SAR patterns in the center of the head were measured for two polarizations (E and H). At all frequencies different SAR distributions are produced for the two polarizations, with the most pronounced difference at 160 MHz. Except at 915 MHz, higher SARs occur for the E-polarization than the H-polarization.

Because of the high values observed, the SAR distribution in the neck area is of particular interest. Maxima in the neck center were found at two frequencies. Much lower SARs were produced in the H-polarization in the neck area.

For the E-polarization the maximum SAR is consistently in the neck, with the highest value at the lowest test frequency of 160 MHz. This observation is consistent with the earlier findings for a homogeneous model. Slight shifts in the actual position of the maximum for the heterogeneous model as compared with the homogeneous model are due to slightly different shapes of the two models.

At all test frequencies the maximum value of the SAR was greater for the heterogeneous model than for the homogeneous model. The difference was relatively small at 160 MHz and 915 MHz, but at 350 MHz the difference was a factor of approximately 10. Intuitively, one may try to explain the increases in the SAR by the smaller cross-sectional area of the neck associated with the heterogeneous model (the neck diameters were 37 cm and 40 cm for the heterogeneous and homogeneous, respectively). However, this is a greatly simplified explanation because of the very complex shape and electrical properties of the models, which in turn make the pattern of the induced electric fields complex.

A more plausible explanation of greater local SARs in the heterogeneous model is the body's smaller size. For the E-polarization at frequencies above resonance, the whole-body average SARs are greater for an ectomorphic and short man than for an average man.

For the H-polarization SAR curves along the mid-plane lack any specific character contrary to the E-polarization. There is a significant increase in the SAR in the head at 160 and 350 MHz for the heterogeneous model as compared with the homogeneous one. The increase is particularly pronounced at 350 MHz.

In the head the SARs were consistently larger for the heterogeneous model. As the conductivity of the brain tissue is 0.62 S/m while the conductivity of the average tissue used in the homogeneous model was 0.93 S/m, that means that the difference in the electric field was

even greater. The shape of the SAR patterns, however, was very similar. The same trend was observed at 160 and 915 MHz.

Local SARs in the heterogeneous and homogeneous models along the direction perpendicular to the body mid-plane and located approximately in the eye socket were also compared for exposures at 160 and 350 MHz in the E-polarization. For the heterogeneous model a well defined "valley" in the SAR patterns can be observed in the vicinity of the nasal bones.

Local SAR distributions in the neck were compared at all test frequencies. For the heterogeneous model the axis of probing was shifted off the center by 1.2 cm in order to by-pass the vertebra. For the homogeneous model the electric field was measured in the center of the neck. At 160 MHz and 350 MHz a well-defined effect of the vertebra can be seen when the shapes of the SAR patterns for the heterogeneous and homogeneous models are compared. At 915 MHz the effect is practically non-existent and the SAR decreases nearly exponentially with distance for both models. Greater values of the SAR in this case can be explained on the basis of larger conductivity of the muscle tissue in this region in the heterogeneous model as compared with conductivity of the average tissue in the homogeneous model.

The SAR patterns at three frequencies along the axis passing through the lung were also compared. It is interesting to note that, except at 160 MHz, the SAR values in the heterogeneous model are higher than in the homogeneous model, even though the conductivities are lower by a factor of approximately two. At 350 and 915 MHz the decrease of SAR with distance is nearly exponential but of different slopes reflecting the differences in the tissue dielectric properties.

Near-Field Exposures

Near-field exposures were performed using resonant dipoles positioned close to the model (less than 0.1 of the wavelength). The local values of the SAR in the mid-plane for a vertical dipole orientation (E-polarization) and a horizontal dipole orientation (H-polarization) were measured. The two orientations may be considered as the two extreme positions of the antennas (i.e., parellel or perpendicular to the length of the body). The SAR along the center axis is consistently greater for the antenna parallel to the body at all test frequencies. The differences in the SAR values for both polarizations are much less along the side of the model and absolute SAR values decrease with increasing frequency.

It was found that most of the energy from resonant dipoles located close to the body is deposited within about 20% of the body volume in the vicinity of the dipole. The SAR values for distances from about 10 to 40 cm from the top of the head are much greater than elsewhere for antennas located at the shoulder level.

The maximum SAR is produced in the neck, as with the far-field exposures. The value of the maximum SAR decreases with frequency from 1 W/kg at 160 MHz, to 0.7 W/kg at 350 MHz and to 0.1 W/kg at 915 MHz for 1 Watt input power to the antenna.

The SAR distributions along the axis perpendicular to the main body axis and located in the chest very close to the center of the antenna varies as follows. Within the first few centimeters from the chest surface upon which the wave is incident (10-15 cm), the SAR decreases nearly exponentially. The attenuation coefficients obtained from fitting a straight line (least-square fit) to the experimental data and the attenuation coefficients calculated for a plane-wave incident upon a muscle equivalent semi-infinite plane are in very close agreement.

The local values of the SAR along the axis penetrating the lung were also measured for the two polarizations. As in the chest, the SAR decreases nearly exponentially along the axis, however, the attenuation coefficient is different due to the different tissue properties and complex path of wave propagation in the near-field of the dipole. The differences in the SAR patterns for the two polarizations appear to decrease as the exposure frequency increases.

The local SARs in the mid-plane were compared for the heterogeneous and homogeneous models at 350 MHz for the E-polarization. There was a small shift in the location of the SAR maximum and in its magnitude. The shift in the location of the maximum SAR was due to the difference in the model size (the homogeneous model was 175 cm tall). Higher maximum SAR for the heterogeneous model is likely partly due to a greater total SAR resulting from the smaller size of the model. However, the difference appears to be too large to be fully accounted for by the size difference.

Similar to the homogeneous model of man, the highest SARs and local "hot spots" were found in the neck of the heterogeneous model.

There is some difference in the shape of the SAR patterns between the heterogeneous and homogeneous models. This difference likely reflects the presence of the spinal cord. The slight shift upwards of the SAR curve at 350 MHz for the heterogeneous model with respect to the homogeneous model reflects the higher conductivity of the muscle tissue in the neck of the heterogeneous model (σ = 1.03 S/m versus the average tissue conductivity σ = 0.93 S/m).

The SAR distribution in the location of the eye, at all three frequencies, for the E-polarization shows an increase of the SAR at locations close to the nasal bones.

Conclusions and Recommendations

A computer-controlled scanning system and miniature, nonperturbing electric field probes were used to acquire maps of spatial distribution of the SAR in a realistic model of man. The model was anatomically correct and reflected electrically heterogeneous composition of the human body. The model was comprised of a simulated skull, spinal cord, rib cage and other major bones as well as brain, lungs and muscle tissue. Electrical properties of the simulated tissues were the same as the electrical properties of corresponding live tissues.

SAR patterns were obtained at three frequencies: 160, 350 and 195 MHz in the far-field and the near-field of resonant dipoles. Resonant dipoles are reasonable models for simulating exposures to hand-held transmitters, and at the same time are amenable for theoretical analyses.

For both the far-field and the near-field, highly nonuniform distributions of the SAR were observed at all three frequencies and for both polarizations investigated (the E and H polarizations). Considerably lower SARs were produced for the H polarization than for the E polarization at 160 and 350 MHz, while comparable SARs resulted from exposures at 915 MHz for both polarizations.

For the far-field exposures, highest local SARs were produced in the center of the neck at 160 and 350 MHz in the E-polarization, while in all other exposure conditions the highest SARs appeared to be produced at the model surface.

The SAR distributions in the heterogeneous model were compared with those in the homogeneous model having average tissue properties. In general, the heterogeneity of the electrical structure was reflected in the SAR patterns at 160 and 350 MHz, but to a lesser extent a

915 MHz. No profound differences in SAR patterns for the two models were noted, although local values differed up to an order of magnitude. In very many locations the values of the SAR for the heterogeneous model were greater than for the homogeneous model. This can be only partly explained by greater average SARs due to a slightly smaller size of the heterogeneous model (162 cm) as compared to the homogeneous model (175 cm).

In the near-field for all test frequencies and both polarizations most of the energy was deposited in about 20% of the total body volume closest to the antenna feedpoint. Higher SARs were produced in most locations under all circumstances tested for the dipole parallel to the long-body axis. Also for the E-polarization high SARs were consistently produced in the neck, both on its surface (at all three test frequencies) and close to the center (except at 915 MHz).

When compared with the homogeneous model, in the near-field as with the far-field, the SAR patterns are quite similar, however inhomogeneity of the model is apparent when it appears close to the path of the electric field probe. In many cases higher SARs, usually two to five times, were measured in the heterogeneous model as compared with the homogeneous model. For many, but not all cases, this can be attributed to the higher conductivity of the tissue (muscle) in the heterogeneous model as compared with the conductivity of the tissue (average) in the homogeneous model.

A comparison of the two models, both in the far- and near-field, leads to a conclusion that a realistic full-scale model is suitable for gaining a general idea about the maximal local and regional SAR values. The locations of the maxima are, however, different for the two models and by inference different from the locations in a living human being since the heterogeneous model only approximates a human being. Nevertheless, the data obtained are useful in assessment of approximate locations of high SARs and their magnitude. The size of the electric field probe (10 mm dia.) and technical limitations such as lack of possibility of measurement of the SAR in bones do not permit obtaining very fine grade patterns.

The results obtained, together with other data previously published, should prove of value in deriving safe exposure limits, in particular for portable transmitters.

Detailed data obtained on the SAR distributions in a realistic heterogeneous model of man at three different frequencies and two polarizations should be used in evaluating numerical methods for calculations of SAR-distributions. This applies to both the far-field and the near-field. Since knowledge of the SAR distribution under various exposure conditions is important in safety considerations, it is essential that there is a reliable and technically convenient method established for gaining such information. The experimental method developed here is highly reliable and relatively accurate (10-15%). However, in view of the technical effort and time required to obtain a complete set of data for any exposure situation, it appears that a numerical method would be preferred, if it can satisfy the requirements of reliability and accuracy.

The results obtained should be used in evaluation of ratios of the local peak to the whole-body average in establishment of safety standards.

Stanislaw S. Stuchly is with the University of Ottawa, Ottawa, Ontario K1N 6N5 Canada.
***Ronald Spiegel** is the EPA Project Officer (see below).*
The complete report entitled "Specific Absorption Rate Distributions in a Heterogeneous Model of the Human Body at Radiofrequencies," (Order No. PB 87-201 356/AS; Cost: $18.95, subject to change) will be available only from:
National Technical Information Service
5285 Port Royal Road
Springfield, VA 22161
Telephone: 703-487-4650
The EPA Project Officer can be contacted at:
Health Environmental Research Laboratory
U.S. Environmental Protection Agency
Research Triangle Park, NC 27711

United States
Environmental Protection
Agency

Center for Environmental Research
Information
Cincinnati OH 45268

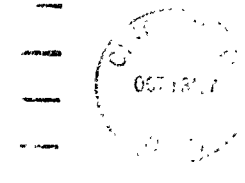

EPA/600/S1-87/003

0000329 PS

U S ENVIR PROTECTION AGENCY
REGION 5 LIBRARY
230 S DEARBORN STREET
CHICAGO IL 60604